

## OPTIMIZATION OF REACTIVE BLACK 5 DYE REMOVAL ONTO KAOLIN FILTER CAKE ACTIVATED CARBON USING RESPONSE SURFACE METHODOLOGY

Amdework Belay<sup>1</sup>, Zemene Worku Negie<sup>1</sup>, Esayas Alemayehu<sup>2,3\*</sup>

<sup>1</sup>Department of Environmental Engineering, College of Engineering, Addis Ababa Science and Technology University, Addis Ababa P.O. Box 16417, Ethiopia

<sup>2</sup>Faculty of Civil and Environmental Engineering, Jimma University, Jimma P.O. Box 378, Ethiopia

<sup>3</sup>Africa Center of Excellence for Water Management, Addis Ababa University, Addis Ababa P.O. Box 1176, Ethiopia

\*Corresponding email: esayas16@yahoo.com, amdeworkb4@gmail.com

**Received:** 07.03.2025; **Accepted:** 23.03.2025; **Available online:** 29.03.2025 **Published:** 30.03.2025

**Cite this article:** Belay, A., Negie, Z. W., & Alemayehu, E. (2025). Optimization of Reactive Black 5 Dye Removal onto Kaolin Filter Cake Activated Carbon Using Response Surface Methodology. *Trends in Ecological and Indoor Environmental Engineering*, 3(1), 36–49.

**Background:** Industrialization consumes a significant amount of water, and the textile sector rapidly expands globally using vast quantities of water. Textile products undergo various procedures such as bleaching, dyeing, printing, and stiffening. Dyeing factories are the major polluters in this industry, generating waste that contains unused organic compounds and colours. Dyes can pose a risk to environmental components and public health, potentially causing harm to vital human organs. Even in small amounts, reactive black 5 dye (RB5) can block light in water, reducing photosynthesis and affecting aquatic plant growth, possibly leading to eutrophication. Prolonged exposure to RB5 has been linked to serious health issues, including skin rashes, cancer, kidney and respiratory failures, and other severe conditions. **Objectives:** The current study aims to establish the effectiveness of using a new, affordable, and environmentally friendly adsorbent, namely kaolin filter cake (KFC), for the removal of reactive black 5 dye from textile wastewater. **Methods:** The prepared kaolin filter cake (KFC) activated carbon was characterized using Fourier Transform Infrared (FTIR), Scanning Electron Microscopy (SEM), X-ray diffraction (XRD), point of zero charge (pHpzc), and Brunauer–Emmett–Teller (BET) surface area. The effectiveness of KFC's decolorization was assessed by adsorption tests that looked at batch process variables, such as pH, adsorbent dosage, contact time, and beginning dye concentration. Response Surface Methodology (RSM) was employed to optimize the RB5 removal. **Results:** The adsorption data closely fit the Langmuir isotherm model, indicating a maximum adsorption capacity of 60.24 mg·g<sup>-1</sup>. Kinetic studies revealed that the adsorption process followed a pseudo-second-order model. Remarkably, KFC demonstrated excellent regeneration potential, retaining 60.52% of its adsorption capacity after five cycles. **Conclusion:** KFC is a highly promising adsorbent with significant potential for sustainable, cost-effective, environmentally friendly, and efficient applications in textile wastewater treatment.

**Keywords:** waste water; organic pollutants; activated carbon; adsorption; kaolin filter cake; optimization; reactive black 5 dye; textile industry.

### INTRODUCTION

Industrialization consumes a significant amount of water, and the textile sector rapidly expands globally using vast quantities of water. Various pollutants released by this industrial sector contaminate freshwater bodies around the world (Gonen & Biçer, 2022). Textile products undergo various procedures such as bleaching, dyeing, printing, and stiffening. Dyeing factories are the major polluters in this industry, generating waste that contains unused organic compounds and colours. Pollution levels are affected by the chemicals and dyes used and their adherence to the fabric (Vojnović et al., 2022). The main contaminant in textile industry effluent is a highly visible dye that can have detrimental toxicological and aesthetic effects even in trace concentrations of less than 1 ppm in the environment (Worku et al., 2023). Dyes may pose health risks, potentially damaging the human vital organs (Hamad & Idrus, 2022). The global market offers around 100,000 distinct kinds of dyestuffs, with an approximate yearly production rate of 700,000 tons. Annually, over a thousand tons of dyes are released into water bodies from various industries, and 45% of this amount is a reactive dye (Kalkan et al., 2014; Nure et al., 2023).

An azo-reactive dye is commonly used in textiles, paper, and cosmetics since it is inexpensive and a vibrant colour (Adamu, 2008). Reactive dyes bind to materials through covalent bonds, enhancing colorization efficiency (Eren & Acar, 2006). However, even in small amounts, reactive black 5 dye (RB5) can block light in water, reducing photosynthesis and affecting aquatic plant growth, possibly leading to eutrophication (Kalkan et al., 2014; Das, & Mishra, 2017). Prolonged exposure to RB5 has been linked to serious health

issues, including skin rashes, cancer, kidney and respiratory failures, and other severe conditions (Dutta, 2013). For these reasons, effectively removing RB5 from wastewater is crucial for environmental health (Eren & Acar, 2006; Obaid & Ali, 2023).

Different methods are employed in the treatment of textile wastewater to eliminate dyes, including chemical oxidation (Alnasrawy, 2023), photocatalytic degradation (Nure et al., 2023), ozonation (Eren & Acar, 2006), coagulation/flocculation (Amin et al., 2015), biological treatment, membrane separation, environmental bacteria, and physical adsorption (Khan & Khan, 2016). Adsorption is an efficient method for textile wastewater removal because of its low operating costs, minimal waste, and simplicity (Ishak et al., 2022). Although activated carbon is widely used for pollutant removal, it is costly and challenging to regenerate (Obaid & Ali, 2023). Consequently, cost-effective alternatives have been explored for removing the RB5, including sugar cane bagasse, red mud, kaolin, rice husk, termite mound, and bentonite (Eren & Acar, 2006; Ishak et al., 2022; Li et al., 2018; Munagapati et al., 2020; Abewaa et al., 2023).

Kaolin filter cake (KFC), a by-product of the Aluminum Sulphate, and Sulphuric acid industry, is mainly composed of aluminosilicate materials of Al<sub>2</sub>O<sub>3</sub> and SiO<sub>2</sub> with a percentage of 75 – 85% and minor oxides (Hamri et al., 2024; Angerasa et al., 2021). KFC is the by-product generated during the filtration unit operation. The improper disposal of KFC waste can lead to environmental and public health (Aragaw & Kuraz, 2018; Mulushewa et al., 2021). Furthermore, several research groups studied the elimination of textile wastewater using clay-based adsorbents such as kaolin, bentonite, metakaolin, modified kaolin, and red mud (Erasto et al., 2023). To the best of our

knowledge, researchers have not studied industrial by-products from KFC as potential adsorbents for removing RB5.

The central aim of this study is to thoroughly investigate KFC's capacity for adsorbing RB5 from textile wastewater. Thus, the study aims to: (i) identify the features and provides a comprehensive description of the crystal structure, surface morphology, functional groups and specific surface area of the adsorbent; (ii) analyse the impact of various experimental parameters on the adsorption percentage of RB5, including pH, adsorbent dosage, contact time, and initial dye concentration; (iii) provide kinetic and isothermal modelling analysis performed using the experimental adsorption data; and finally (iv) optimize the adsorption process using a central composite design (CCD) within the framework of response surface methodology (RSM).

## MATERIALS AND METHODS

### Materials and chemicals

The adsorbent was prepared using various mechanical size reduction tools, including jaw crushers, disk mills, and mortars,

as well as traditional thermal equipment like muffle furnaces and hot air ovens. For the batch adsorption experiments, a range of analytical tools and glassware were typically employed, such as pipettes, test tubes, centrifuges, magnetic stirrers, pH meters, and measuring cylinders. During the batch experiments, sodium hydroxide, concentrated sulfuric acid, and RB5 were used to create the synthetic dye solution and to adjust the pH.

### Preparation of adsorbents

KFC was collected from the Awash Melkassa Chemical Factory in Awash, Ethiopia. The plant comprises five primary units: filtration, evaporation, crystallization, grinding, and neutralization. During the operation of the filtration machine, the by-product known as KFC was produced. To process the KFC, a grinder, a disk mill, electrical sieves with mesh sizes less than 0.075 mm, and a muffle furnace were used for crushing, grinding, and sieving the collected filter cake. The KFC was then treated at 700 °C for two hours to produce the calcined adsorbent. A schematic representation of the adsorbent preparation for both the raw KFC (RKFC) and calcined KFC (CKFC) samples is shown in Figure 1.

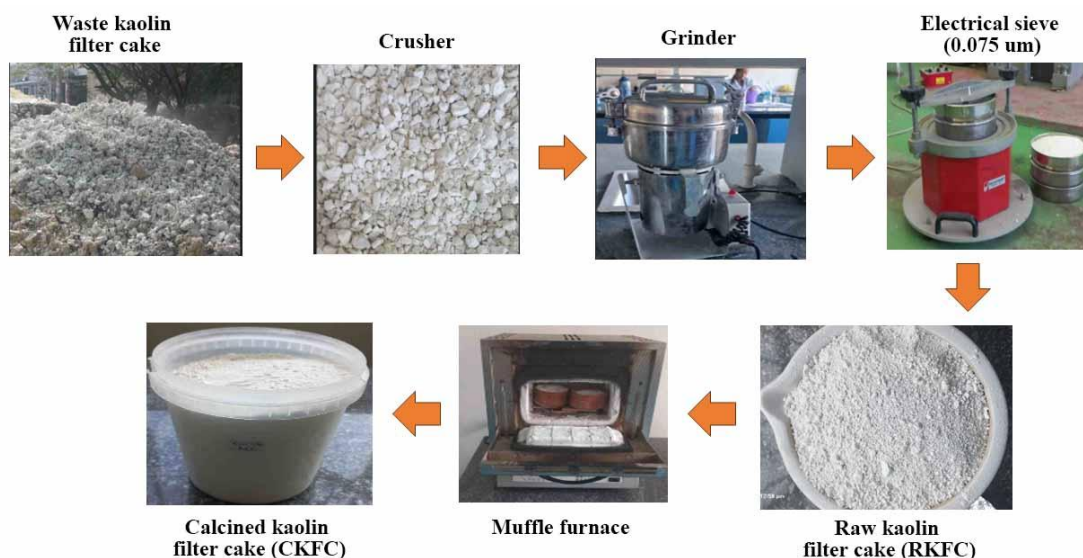


Figure 1. A schematic representation of the adsorbent preparation

### Preparation of RB5 solutions

Every chemical utilized in the experiment was analytical grade and unpurified. Kombolcha Textile Share Company, an export-focused textile plant situated in the Amhara region of Kombolcha, approximately 380 km northeast of Addis Ababa, Ethiopia, provided RB5 (MF: C<sub>26</sub>H<sub>21</sub>N<sub>5</sub>Na<sub>4</sub>O<sub>19</sub>S, MW: 991.8 g/mol). This dye is used extensively in the dyeing process in the textile industry. A stock dye solution of 1000 mg/L (1.0 g diluted in 1000 mL) was prepared and used to create the required concentration. The anionic RB5's  $\lambda_{max}$  was 597 nm (Ishak et al., 2022).

### Adsorbent characterization

By utilizing the salt addition method, we can accurately determine the point of zero charge (PZC). To effectively raise the initial pH from 2 to 10, we strategically added 0.01 M HCl and 0.01 M NaOH as needed. Each flask received 0.5 g of KFC adsorbent and the solution was vigorously agitated at room temperature 25 °C for 36 hours, maintaining a consistent speed of 150 rpm on an orbital shaker to ensure optimal mixing and effectiveness. After recording the final pH, the pH change (pH<sub>f</sub> – pH<sub>i</sub>) was calculated. The PZC was then determined by

plotting a graph and finding the x-intercept (Amin et al., 2015; Fito et al., 2023).

### Brunauer, emmett, and teller (BET)

The surface area determination was conducted using the Brunauer, Emmett, and Teller method as follows: Approximately 4 g of activated carbon were placed in three degassed sample tubes and subjected to heating at 100 °C for 2 hours. Subsequently, the surface area was assessed by analysing the adsorption and desorption of nitrogen (N<sub>2</sub>) gas at an atmospheric pressure of 700 mm, utilizing a surface area analyser (SA-9600, Horiba, Japan) (Amin et al., 2015; Alemayehu et al., 2017).

### Scanning electron microscope (SEM)

A scanning electron microscope was employed to investigate the morphological characteristics of the KFC. The morphological features of both the raw and calcined KFC were evaluated at various resolutions. A small quantity of the adsorbent was positioned on the sample holder coated within the vacuum chamber of the SEM and analysed under the specified conditions. Adherence to standard operating procedures for the examination of surface morphologies with

the JCM-6000PLUS BENCHTOP SEM (JEOL, Japan) was maintained throughout the preparation and scanning of both samples, which were operated at a voltage of 5.00 kV (Carmen & Daniela, 2012; Hassan et al., 2022).

### Fourier transform infrared (FTIR)

The Fourier Transform Infrared spectrophotometer was employed to identify the functional groups present in the adsorbent. The analysis was conducted on the functional groups of the adsorbents before and following the adsorption process, utilizing the FTIR spectrophotometer (Shimadzu IRAffinity-1s, Japan) across a spectral range of 4000 to 400 cm<sup>-1</sup>.

### X-ray diffraction (XRD)

The X-ray diffraction (XRD) technique was utilized to characterize the crystalline nature of the adsorbent using an XRD instrument (Olympus BTXH, Japan). This analysis sought to identify the presence of both amorphous and crystalline structures within activated carbon (AC) by measuring the diffraction angle (2θ) ranging from 5 to 90 degrees. The X-ray system was operated at a current of 15 mA, utilizing Cu Kα radiation at a voltage of 40 kV/40 mA.

### Batch adsorption experiment

Adsorption experiments were conducted through a batch experimental technique. This study aimed to investigate the adsorption capacity of the anionic RB5 in an aqueous solution utilizing KFC as the adsorbent. The experimental procedures were performed in a closed beaker equipped with a magnetic stirrer. Several parameters were analysed, including pH levels (ranging from 3 to 9), adsorbent dosage (between 2.5 and 4.5 g), contact time (evaluated within a range of 40 to 80 min), and the initial concentration of RB5 (ranging from 80 to 160 mg/L). Upon completion of each experiment, the resulting supernatant was analysed using a visible spectrophotometer

at the specific wavelength corresponding to RB5. The quantification of the amount and percentage of RB5 ions adsorbed by KFC was achieved through the application of Equations (1) and (2) (Hasan et al., 2024).

$$R (\%) = \frac{(C_0 - C_e)}{C_0} \cdot 100, \quad (1)$$

$$q_e \left( \frac{\text{mg}}{\text{g}} \right) = \frac{(C_0 - C_e)}{m} \cdot v, \quad (2)$$

where R is the percentage removal; q<sub>e</sub> is the uptake capacity; C<sub>0</sub> and C<sub>e</sub> are initial and equilibrium concentrations of RB5 in the solution, mg/L; m is the adsorbent mass, g; v is the volume of the solution, L.

### Optimization of RB5 adsorption

The response surface methodology (RSM) Central Composite Design (CCD) technique was used to examine the influence of certain factors on the adsorption process. The RSM is a helpful statistical technique for designing experiments (DOE) and optimizing a variety of parameters (Mutambyi et al., 2023). The empirical equation 2n + 2n + c served as the basis for 30 tests generated by the RSM-CCD in Design Expert® software version 13.0. where "n" is the number of independent parameters and "c" is the number of centre point experiments. Equation (3) provided a quadratic model for the analysis of response surface regression for the design response.

$$y = b_0 + \sum_{i=1}^K b_i X_i + \sum_{i=1}^K b_{ii} X_i^2 + \sum_{i=1}^K \sum_{j=1}^K b_{ij} X_i X_j + \varepsilon \quad (3)$$

where y is the response variable; b<sub>0</sub> is the intercept constant; K is the number of variables; b<sub>i</sub> are the coefficients of linear parameters; ε is the between the calculated and experimental results; X<sub>i</sub> and X<sub>j</sub> are variables; b<sub>ii</sub> is the coefficient of quadratic parameters; b<sub>ij</sub> is the coefficient of the interacting parameters. Table 1 gives the levels of each parameter for this study.

Table 1. Adsorption factors and corresponding levels for RSM-CCD experiments

Factors	Factor symbol	Unit	Levels	
			Lower	Upper
pH	A	–	3	9
Adsorbent dose	B	g	2.5	4.5
Contact time	C	min	40	80
Initial RB5 concentration	D	mg/L	80	160

### Adsorption phenomenon study

Isotherm models are utilized to describe the equilibrium between the quantity of adsorbate adsorbed onto the surface of an adsorbent and the concentration of the adsorbate in a solution. Among the various adsorption isotherms, the Freundlich and Langmuir models are the most widely recognized. The Langmuir adsorption isotherm, in particular, is well suited for monolayer adsorption as it posits that adsorption occurs at specific, uniform sites on the adsorbent's surface (Seleman et al., 2023). The Freundlich adsorption isotherm model indicates that the formation of multilayer and heterogeneous systems is attributed to the non-uniform distribution of adsorption affinities, rather than being confined to single-layer formation (Srivastava et al., 2022).

Equation (4) represents the linear form of Langmuir's isotherm used to determine the adsorption parameters.

$$\frac{1}{q_e} = \frac{1}{KLq_{\max}} \cdot \frac{1}{C_e} + \frac{1}{q_{\max}}, \quad (4)$$

where q<sub>max</sub> is represents the maximum adsorption capacity, mg/g; q<sub>e</sub> is the uptake capacity; KL is Langmuir's isotherm

constant, which shows the binding affinity between dye and KFC, L/mg.

Equation (5) represents the linear form of Freundlich's isotherm:

$$\text{Log}q_e = \text{Log}K_f + \frac{1}{n} \text{Log}C_e, \quad (5)$$

where K<sub>f</sub> is Freundlich's constant and is used to measure the adsorption capacity, and  $\frac{1}{n}$  is the adsorption intensity,  $\frac{1}{n}$  demonstrates the adsorption process is either favourable ( $0.1 < \frac{1}{n} < 0.5$ ) or unfavourable ( $\frac{1}{n} > 2$ ).

The kinetics rate at which the adsorbate (RB5) was adsorbed on the surface of the adsorbent (CKFC) was investigated using pseudo-first-order and second-order kinetic models. These kinetics models demonstrate the adsorbent's effectiveness by displaying how quickly or slowly it adsorbs the adsorbate.

The pseudo 1st order is represented in Equation (6):

$$\ln(q_e - q_t) = \ln q_e + K_1 \cdot t, \quad (6)$$

where q<sub>t</sub> represents the adsorption capacity at time t, mg/g; K<sub>1</sub> is the equilibrium rate constant, min<sup>-1</sup>.

Pseudo 2nd order is represented in Equation (7):

$$\frac{t}{q_e} = \frac{1}{K_2 q_e^2} + \frac{1}{q_e} \quad (7)$$

where  $K_2$  is the equilibrium rate constant,  $g \cdot mg^{-1} \cdot min^{-1}$ . The values of linear coefficient regression ( $R^2$ ) were used to predict the most suited isotherm and kinetic model for the adsorption process (Hasan et al., 2022).

### Regeneration of adsorbent

Evaluating the potential for regeneration and reuse is crucial for demonstrating the usefulness and sustainability of adsorbents. To recycle the adsorbent once the adsorption equilibrium is reached, it is necessary to desorb the adsorbed molecules. In the studies conducted, 3.5 g/L of dye-loaded KFC (Kinetic Activated Carbon) was agitated for two hours at 180 rpm in 100 mL of 0.1 M hydrochloric acid (HCl). After this process, the dye-loaded KFC was rinsed with deionized water and dried in an oven at 80 °C for one hour before being reused. The effectiveness of the KFC adsorption was tested over five cycles using this procedure (Abdu et al., 2024).

## RESULTS AND DISCUSSIONS

### Characteristics of a KFC adsorbent

#### The point of zero charge (pHpzc)

An important factor in understanding surface-active centres and binding capabilities is the point of zero charge (pHpzc), which is the pH level at which an adsorbent exhibits a neutral surface charge. Higher pH values than the PZC are preferable for adsorbing cationic dye, whereas lower pH levels than the PZC are better for anionic dye adsorption techniques.

The pHpzc value of KFC is 7.1 (Figure 2), indicating that it has a positive charge at pH values lower than 7.1. This characteristic makes KFC useful for anionic dye adsorption (Magdy et al., 2017). Consequently, negatively charged dyes, such as RB5, are better absorbed at pH values lower than pHpzc. Research indicates that RB5 performs best at

a pH range of 4 to 6, which is below the pHpzc, suggesting a higher binding affinity at these levels (Hamri et al., 2024).

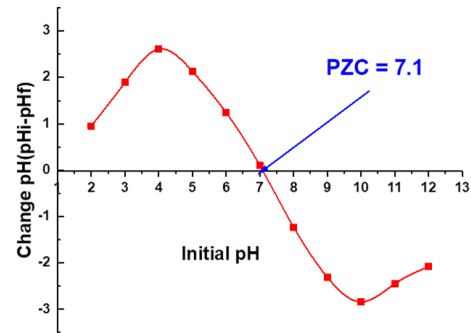


Figure 2. Point of Zero charges for calcinated kaolin filter cake (CKFC)

### Brunauer-Emmett-Teller (BET) surface area analysis

Measuring the specific surface area (SSA) is essential for describing the characteristics of materials, particularly in fields like material science, adsorption, and catalysis (Ribeiro et al., 2022). The Brunauer-Emmett-Teller (BET) method is frequently used because it is reliable when evaluating SSA, especially in porous materials (Azha et al., 2021). This approach produces adsorption isotherms by assessing the nitrogen gas adsorption at different pressure levels. It was discovered that the BET of the activated KFC adsorbent was 36 m<sup>2</sup>/g and that of the studded raw KFC adsorbent was 19 m<sup>2</sup>/g (Souhassou et al., 2024). The produced CKFC has a large specific surface area, a huge pore volume, and a high degree of porosity, as indicated by the data above. It also offers a significant number of active sites that may interact with RB5 molecules, increasing its adsorption capability.

### Scanning Electron Microscopy (SEM) Analysis

SEM Analysis was utilized to investigate the morphology of the RKFC and CKFC adsorbents, as shown in Figure 3a and 3b.

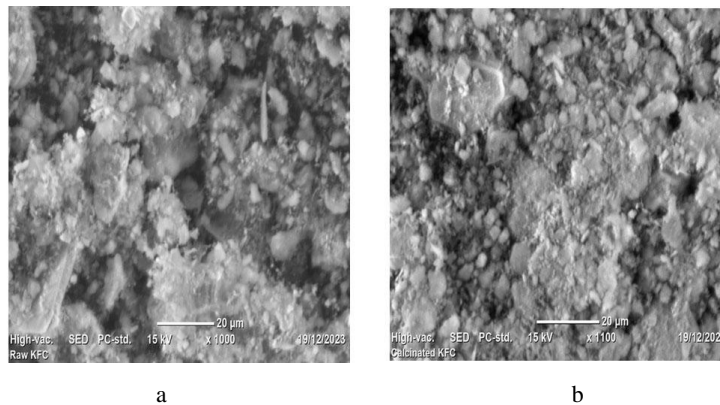


Figure 3. SEM analysis: a – raw kaolin filter cake; b – calcinated kaolin filter cake

The images reveal a porous surface with irregular shapes and unstructured regions characterized by uneven edge aggregation. This analysis highlighted the differences in surface morphologies and porosity between the two adsorbents. The CKFC adsorbent exhibits a greater surface area and porosity, which can be attributed to its preparation and activation procedures. This phenomenon, where the activated adsorbent shows a significantly larger surface area, has also been documented in the physicochemical properties of kaolin clay (Aragaw & Kuraz, 2018; Slatni et al., 2020). The micrograph showed a structure with significant porosity, which was marked by a diverse range of sizes and shapes that were irregular. This

allows for the successful and efficient adsorption of various sizes of adsorbates. The surface magnification for both raw and activated kaolin filter cake (KFC) was set at 20 µm. As illustrated in Figure 3a, the pore openings on the sorbent surface of the raw kaolin filter cake are not consistently visible. The distinct layered rectangular shape indicates that the natural kaolinite, which is untreated, consists of a double layer of aluminosilicate clay, which could be identified as RKFC (Ike et al., 2024).

Additionally, the calcined kaolin exhibits a complex structure characterized by its adsorptive properties and porosity. The photograph indicates that the calcined adsorbents display more agglomerated and less structured morphologies. As shown in

Figure 3b, the calcined adsorbent has significantly more available pores. Consequently, these adsorptive properties enhance the effective adsorption of RB5 ions from the solution (Slatni et al., 2020; Johin et al., 2024).

### Fourier Transform Infrared (FTIR) analysis

Figure 4 presents the results of an analysis of the FTIR surface functional group properties of the CKFC sorbent and the powder adsorbent loaded with adsorbate RB5 in a spectrum, typically from 4000  $\text{cm}^{-1}$  to 400  $\text{cm}^{-1}$ . The produced CKFC adsorbent contains hydroxyl groups  $\text{OH}^-$  from  $\text{Si-OH}$  and  $\text{AlOH}$ , which can create connections between the tetrahedral and octahedral sheets of kaolinite. This is indicated by a small peak at 3610  $\text{cm}^{-1}$  (Ike et al., 2024). The peaks observed in the spectrum at 3450 and 1624  $\text{cm}^{-1}$  correspond to the tension vibrations of  $\text{OH}^-$  groups and the bending band of water molecules, respectively (Aragaw & Alene, 2022). Stretching vibrations of aluminum oxide suggest that  $\text{Si-O}$  is the main constituent of the kaolin under study, and the absorption peaks at 1112, 1020, and 756  $\text{cm}^{-1}$  are thought to be caused by  $\text{Si-O}$  (Li et al., 2021). The peaks at roughly 558 and 462  $\text{cm}^{-1}$ , respectively, show the bending vibrations of  $\text{Si-O-Si}$  and  $\text{Si-O-Al}$  (Angerasa et al., 2021).

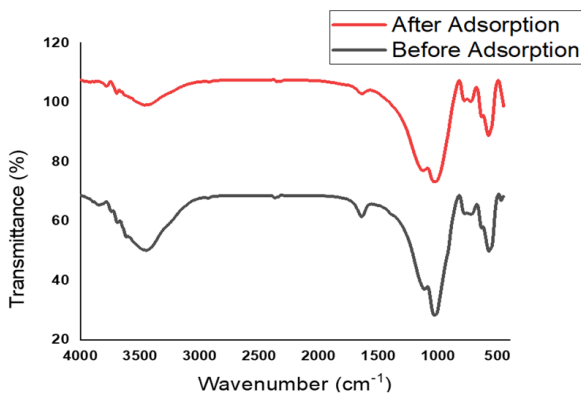


Figure 4. FTIR analysis for Calcined kaolin filter cake before and after adsorption

The characteristic absorption peaks of kaolin adsorbent and the adsorbent-loaded dyes RB5 showed no significant variation in percentage transmittance, indicating that the basic structure remained unchanged during the interactions between the adsorbent and dyes (Aragaw & Alene, 2022). Minor shifts and changes in the positions and intensities of peaks were observed, influenced by the number of adsorbed dye molecules. These variations can impact the percentage transmittance. The slight shifts in position are associated with the surface properties and the interactions of the adsorbent and the functional groups present on the RB5's surface. These interactions may arise from electrostatic forces or weak van der Waals forces, as the dye has ionic characteristics when in solution. Additionally, these observed shifts are a result of the physical relationship with the dye and the adsorbent at their surfaces (Hamri et al., 2024; Caponi et al., 2017).

A significant indicator of the adsorbate load is the change in peak intensity or the bend in shape seen before and following the adsorption of dye onto the surface of the adsorbent. The adsorbent's bending shape's percentage transmittance was at its highest before the sorption process, indicating that dye ions unoccupied the adsorbent's surface. However, after the adsorption process, the percentage transmittance of the bending shape decreased significantly, suggesting that the surface was occupied by the dyes, which blocked the infrared signals.

### Analysis of X-ray diffraction (XRD) results

Analysis of XRD was conducted on the raw RKFC and CKFC samples to verify the conversion to an amorphous state. Figure 5 shows that the RKFC contains three phases: illite, quartz, and kaolinite, with kaolinite identified by reflections at  $2\theta$  angles of 12.3°, 20.3°, and 24.8°, and illite at 23.05°, 29.8°, and 47.4°. The pre-treated RKFC displays several peaks, indicating crystalline phases. In contrast, the calcinated sample has a broad hump around 26°, confirming that heating at 700 °C for 2 hours and rapid quenching transformed the crystalline phases into an amorphous state, as noted in previous studies (Aragaw, 2020). The calcination stage was effective, leading to the de-hydroxylation step that damaged the kaolinite surface structure. As a result, an amorphous material was recognized by its rise displayed on the diffractogram background, as already discussed (Li et al., 2021; Kassa et al., 2022).

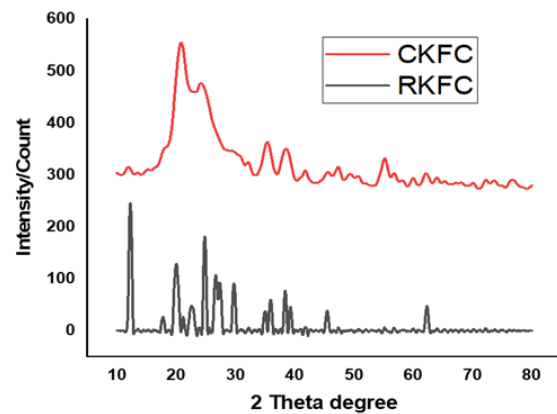


Figure 5. XRD result: a – raw adsorbent; b – calcined adsorbents

The study involved the production of amorphous silica through the calcination of filter cake at 700 °C for 2 hours, following water cooling. The same finding has been observed for metakaolin materials, which exhibited higher free energy and pozzolanic characteristics, turning them into the most reactive clay (Kassa et al., 2022). Metakaolin clay has strong reactivity and is appropriate for applications in the production of binding materials, due to its reduced content of illite and quartz (Mustapha et al., 2021). Results of XRD of the raw and calcined kaolin filter cake adsorbent in this study resemble those found in earlier research.

### Effect of individual factors on RB5 removal

The main adsorption parameters investigated include adsorbent dose, contact time, pH, and initial RB5 concentration. These parameters were analyzed by the one-factor-at-a-time method to assess their effects on the sorption process. The pH levels were varied from 3.0 to 9.0, the adsorbent dose was adjusted between 2.5 to 4.5 g, the contact time was set within a range of 40 to 80 min, and the initial RB5 concentration (80 to 160 mg/L). The effects of each parameter on the adsorption process are illustrated in Figures 6a to 6d.

### Effect of pH

In any adsorption study, the pH factor is an important parameter. As shown in Figure 6a, the highest retention rate is achieved at acidic pH levels, particularly starting from a pH of 4. In contrast, the sorption capacity of RB5 decreases slightly at alkaline pH. The explanation for this decline is that when the pH falls below the point of zero charge ( $\text{pH}_{\text{pzc}}$ ), extra  $\text{H}^+$  ions occupy some adsorption sites at acidic pH values, leading to a positively charged clay surface (Worku et al., 2023;

Abdu et al., 2024). The adsorbent surface exhibits a positive charge at lower pH levels, which enhances the electrostatic attraction with the negatively charged RB5. This observation aligns qualitatively with findings from other researchers and is supported by the outcomes related to the (pHzpc) (Kosmulski, 2021).

### Effect of sorbent dose

The amount of adsorbent used is a crucial factor because it determines the adsorbent's ability to handle a specific initial

concentration. As shown in Figure 6b, the sorption rate of the RB5 increased with a higher mass of adsorbent. This increase can be attributed to a greater number of available adsorption sites as the adsorbent dosage rises (Farrokhzadeh et al., 2020). As the dose of adsorbent used exceeds 4.5 g/L, the extracted dyes remain largely unchanged. At a dye concentration of 120 mg/L, it appears that when the dosage surpasses 3.5 g, the available adsorbate molecules are already saturated, resulting in the removal efficiency stabilizing at a constant level (Nure et al., 2023).

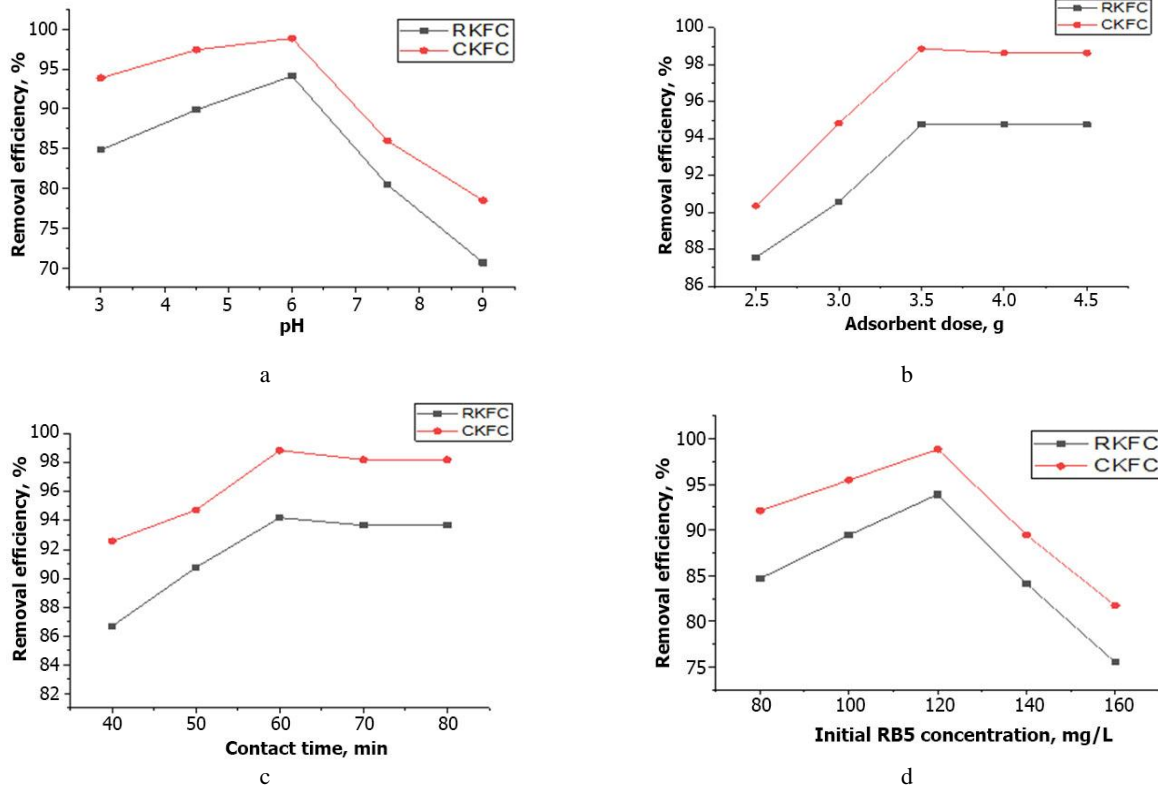


Figure 6. Effect on removal efficiency percentage: a – pH; b – adsorbent dose; c – contact time; d – dye concentration

### Effect of contact time

The study investigated the removal of RB5 through adsorption using KFC material over time. Figure 6c illustrates the effect of time on the dye solution during batch mode adsorption. It was observed that equilibrium is reached after 60 min, at which point the rate of adsorption stabilizes following an initial rapid increase. The rise in removal percentage over time suggests that adsorption is a process that requires time to occur. According to the previous study, the adsorption mass transfer phenomenon consists of three main steps: external diffusion, internal diffusion, and attachment to the active site. Consequently, there is a certain time required to adsorb a specified amount of adsorbate until all available surface sites are occupied or equilibrium is reached. The presence of many free active sites at the beginning of the adsorption may have influenced this outcome. Depending on the kinds of sorbent and dye being utilized, as well as their adsorption behavior, the amount of time required to efficiently remove the majority of the dye may be short or long (Angerasa et al., 2021).

### Effect Initial RB5 concentration

The efficiency of the CKFC for adsorbing RB5 is influenced by the initial dye concentration. As shown in Figure 6d, increasing RB5 concentration from 80 to 120 mg/L enhances the dye's sorption capacity until saturation is reached. Once saturated, no

further adsorption takes place because the binding sites for the dye are fully occupied. Conversely, as the concentration increases, the dye's adsorption capacity may decline due to the early saturation of the adsorbent's surface sorption sites. The saturation of these active sites leads to a reduction in removal effectiveness at higher dye concentrations (Ike et al., 2023).

### RSM model fitting and summary statistics

To optimize the removal of RB5 from textile industrial wastewater, we examined the effects of four key factors: initial dye concentration, contact time, pH, and adsorbent dosage. We analysed the independently selected factors by utilizing the RSM design combinations derived from a Central Composite Design (CCD) with Design Expert 13 software. In this study, we focused on four factors at three levels using CCD to assess and improve the CKFC preparation process variables for the RB5 textile dye removal. As shown in the Table 2, we conducted a total of 30 experimental runs for the RSM analysis. The actual and predicted percentages of RB5 removal are provided in Table 2.

### Analysis of variance

The summary was generated utilizing a quadratic model from Design-Expert version 13.0, as shown in Table 3. ANOVA was applied to evaluate model fit and compare various models through sequential sums of squares. A comprehensive analysis of model statistics was conducted to determine the

effectiveness of different models regarding the percentage removal efficiency of RB5 by the CKFC adsorbent. The model's F-value of 306.99 indicates that the proposed model is statistically significant, with only a 0.01% likelihood that an F-value of this magnitude would arise due to random

variation. Furthermore, the lack of fit was determined to be insignificant, exhibiting an F-value of 1.68. This insignificance in the lack-of-fit test reinforces the adequacy of the proposed model, suggesting a 29.4% probability that an F-value this large for lack of fit could occur purely by chance.

Table 2. The experimental and predicted values of RB5

Run	A: pH	B: Adsorbent dose, g	C: Time, min	D: Initial RB5 concentration, mg/L	RB5 removal, %	Predicted RB5 removal, %
1	4	4.5	40	80	89.78	90.12
2	8	4.5	80	80	86.36	86.58
3	8	4.5	40	160	82.93	82.76
4	6	3.5	60	120	98.87	98.22
5	6	3.5	60	120	98.16	98.22
6	8	4.5	40	80	88.31	88.68
7	8	2.5	40	160	79.92	80.09
8	6	3.5	60	200	85.48	86.35
9	4	4.5	80	160	91.68	91.37
10	8	2.5	80	160	83.67	83.04
11	4	2.5	40	80	90.64	90.87
12	4	4.5	80	80	90.73	90.77
13	6	3.5	20	120	92.58	92.40
14	4	2.5	40	160	88.36	87.86
15	6	3.5	60	120	97.94	98.22
16	4	4.5	40	160	86.95	86.77
17	6	3.5	60	120	97.63	98.22
18	6	1.5	60	120	88.43	88.69
19	8	2.5	40	80	85.65	85.67
20	4	2.5	80	80	92.74	92.62
21	6	3.5	60	40	92.12	91.33
22	6	3.5	60	120	98.48	98.22
23	6	3.5	100	120	95.74	96.00
24	4	2.5	80	160	93.73	93.56
25	6	5.5	60	120	89.68	89.50
26	8	2.5	80	80	84.28	84.67
27	6	3.5	60	120	98.21	98.22
28	2	3.5	60	120	83.56	83.86
29	8	4.5	80	160	84.64	84.61
30	10	3.5	60	120	72.12	71.90

Table 3. ANOVA for the RSM quadratic model

Source	Sum of squares	df	Mean square	F-value	p-value	Note
Model	1151.68	14	82.26	306.99	< 0.0001	Significant
A: pH	214.38	1	214.38	800.03	< 0.0001	
B: Adsorbent dose	0.9963	1	0.9963	3.72	0.0730	
C: Time	19.46	1	19.46	72.61	< 0.0001	
D: Initial RB5 concentration	37.23	1	37.23	138.92	< 0.0001	
AB	14.16	1	14.16	52.83	< 0.0001	
AC	7.58	1	7.58	28.27	< 0.0001	
AD	6.59	1	6.59	24.60	0.0002	
BC	1.22	1	1.22	4.54	0.0502	
BD	0.1139	1	0.1139	0.4251	0.5243	

A non-significant lack of fit is preferred because it shows that the model fits the data well. Model terms are considered significant when the P-values < 0.05. The relationship between the input variables and the percentage of RB5 removal, in terms

of both coded and actual factors, is demonstrated in the equations resulting from the analysis of the observed data using the Central Composite Design (CCD).

The final equation in terms of coded factors:

$$Y = 98.215 - 2.98875A + 0.2038B + 0.900417C - 1.24542D + 0.940625AB - 0.688125AC - 0.641875AD + 0.989375CD - 5.08385A^2 - 2.2801B^2 - 1.00385C^2 - 2.34385D^2 \quad (8)$$

In this context, Y represents the percentage of RB5 removal, while A denotes the pH level, B is the adsorbent dose, C indicates the contact time, and D refers to the initial dye concentration. The terms AB, AC, AD, CD, A<sup>2</sup>, B<sup>2</sup>, C<sup>2</sup>, and D<sup>2</sup> represent the interaction effects between pH and adsorbent dose, pH and contact time, pH and initial dye concentration, contact time and initial concentration, as well as the squared terms for contact time, pH, initial concentration, and adsorbent dose, respectively. In the equation, positive coefficients indicate a synergistic effect, whereas negative coefficients suggest an antagonistic effect. The standard deviation for Equation (8) is 0.5177, indicating that the predicted values align closely with the actual values, suggesting high accuracy. In this model, the terms A, C, D, AB, AC, AD, CD, A<sup>2</sup>, B<sup>2</sup>, C<sup>2</sup>, and D<sup>2</sup> are considered significant. However, the interaction terms BC and BD are deemed insignificant (P > 0.05).

Consequently, to enhance the model's accuracy, these insignificant interaction terms were removed from the equation.

### Evaluation of RSM model results

Regression coefficients were utilized to assess the fit of linear, quadratic, and cubic models (R<sup>2</sup>). As indicated in Table 4, the cubic model was found to be aliased. The quadratic regression model, which had an R<sup>2</sup> value of 0.9965, provided the best fit for the experimental data. Consequently, the removal rate of RB5 was predicted using this quadratic model.

The predicted R<sup>2</sup> value of 0.9834 is reasonably close to the adjusted R<sup>2</sup> value of 0.9933, with a difference of less than 0.2. Adequate precision measures the signal-to-noise ratio, and a ratio greater than 4 is considered desirable. Your ratio of 71.886 indicates a strong signal, as shown in Table 5. Therefore, this model can effectively be used to navigate the design space.

Table 4. Model Summary Statistics

Source	Std. dev.	R <sup>2</sup>	Adjusted R <sup>2</sup>	Predicted R <sup>2</sup>	Press	Note
Linear	5.95	0.2354	0.1131	-0.0066	1163.30	
2FI	6.64	0.2746	-0.1072	-0.1979	1384.42	
Quadratic	0.5177	0.9965	0.9933	0.9834	19.18	Suggested
Cubic	0.4108	0.9990	0.9958	0.9663	38.96	Aliased

Table 5. Fit statistics

Std. dev.	Mean	C.V., %	R <sup>2</sup>	Adjusted R <sup>2</sup>	Predicted R <sup>2</sup>	Adeq. precision
0.5177	89.65	0.5774	0.9965	0.9933	0.9834	71.8857

### Residual plots for response yield

Figure 7a displays a linear plot of the normal probability where the residual studentization is contrasted with the residual variance, indicating that the data follows a normal distribution. If the data were not linear, the underlying model's assumptions would be violated, resulting in certain error terms becoming irregularly distributed. In Figure 7b, when the residuals are plotted against the predicted responses, it shows that the residuals are randomly dispersed. Figures 7c and 7d illustrate a high level of conformity between the observed data and the predicted values, so validating the applicability of the model (Bello et al., 2023).

### The interaction effects and parameter optimization

In this research, three-dimensional response surface plots (3D) along with relevant contour plots utilizing the RSM model to examine the interactive impacts of chosen variables on dye removal percentage were developed. Specifically, we aimed to determine the optimal values for each factor to maximize the removal efficiency of the RB5. Out of the six interactions examined, four were found to be statistically significant. These significant interactions include: AB: the interaction between pH and adsorbent dose, AC: pH and contact time, AD: pH and the initial concentration of RB5, CD: contact time and the initial RB5 concentration.

### Adsorbent dose and pH

The interaction effect of pH and adsorbent dose on the removal of RB5, conducted at a constant contact time of 60 min and an initial RB5 concentration of 120 mg/L, is illustrated through contour and 3D plots, as depicted in Figure 8. The percentage of dye removal of the CKFC adsorbent for dye molecules increases with the adsorbent dose and decreases with pH. This trend suggests that a higher

amount of adsorbent creates more opportunities for dye molecule adsorption until the process reaches equilibrium. The maximum RB5 removal achieved in the experiment was 98.87%, while the predicted removal percentage was 98.22%. This indicates that the predicted and experimental removal percentages are in good correlation.

### pH and contact time

The interaction of initial concentration and time on the removal efficiency of RB5 at a fixed pH of 6 and a dose of 3.5 g is illustrated through 3D and contour plots, as shown in Figure 9. Removal efficiency increases significantly as the adsorption time rises from 40 to 60 min and the pH decreases from 8 to 4. This increase in removal efficiency under these specific conditions can be attributed to the favourable environment that allows for rapid mass transfer due to the increased contact time and lower pH. Additionally, it appears that the bio-sorbent, which was activated, provided sufficient surface area to effectively take up the dye molecules. However, as the process approached equilibrium, the rate of adsorption began to slow, resulting in the removal efficiency stabilizing at a nearly constant level (Njuhous et al., 2023).

### pH and initial RB5 concentration

The interaction of pH and RB5 concentration on the removal percentage of CKFC adsorbent during the adsorption of dye molecules is illustrated in Figure 10. As anticipated, the removal percentage is more significantly affected by the dye concentration when the time is held constant at 60 min and the adsorbent dosage is maintained at 3.5 g. The removal efficiency increased to 95.8% when the dye concentration was reduced to 120 mg/L, with the adsorbent amount still set at 3.5 g. A higher RB5 concentration can exceed the available surface area of the 3.5 g of adsorbent; consequently, some dye molecules may remain unremoved from the synthetic solution.



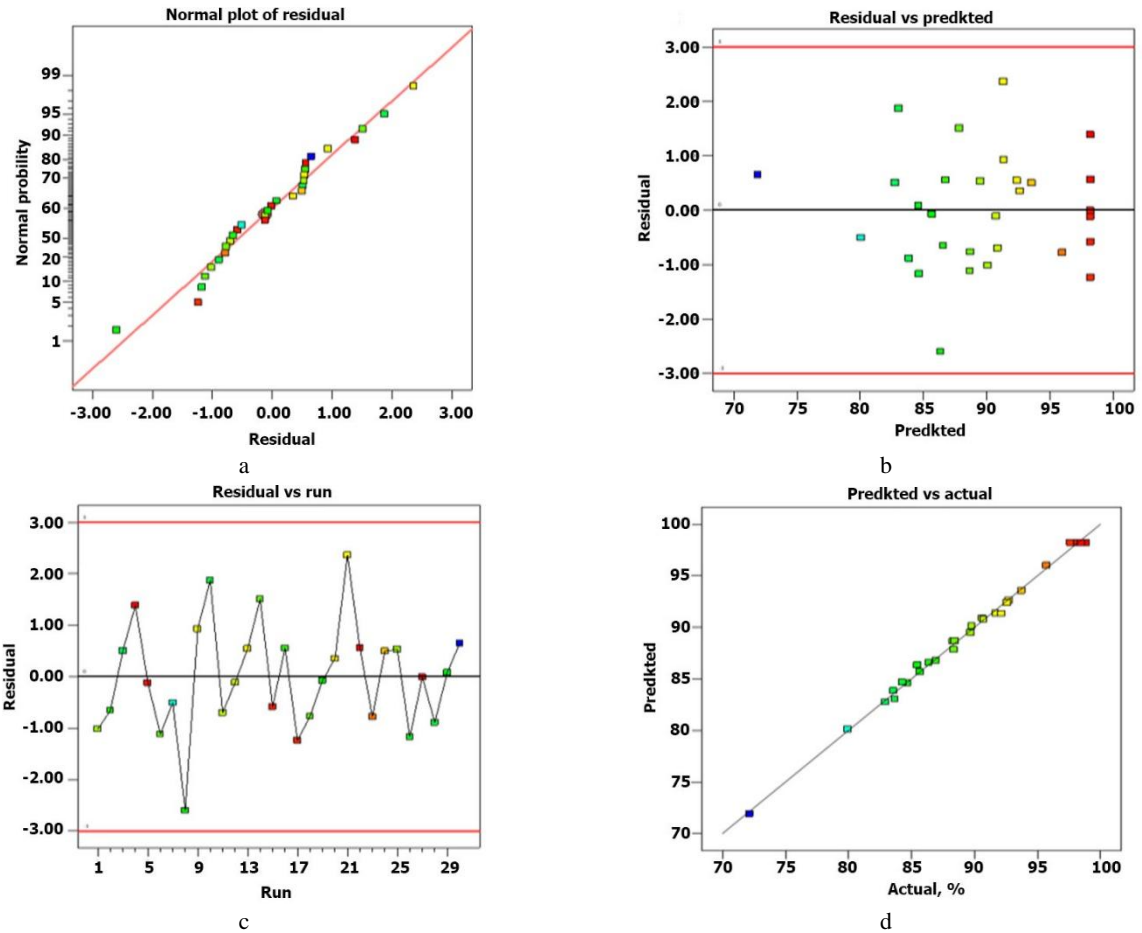


Figure 7. Residual plots of response yield: a – normal plots of residuals; b – residual vs predicted; c – residuals vs run; d – predicted vs actual

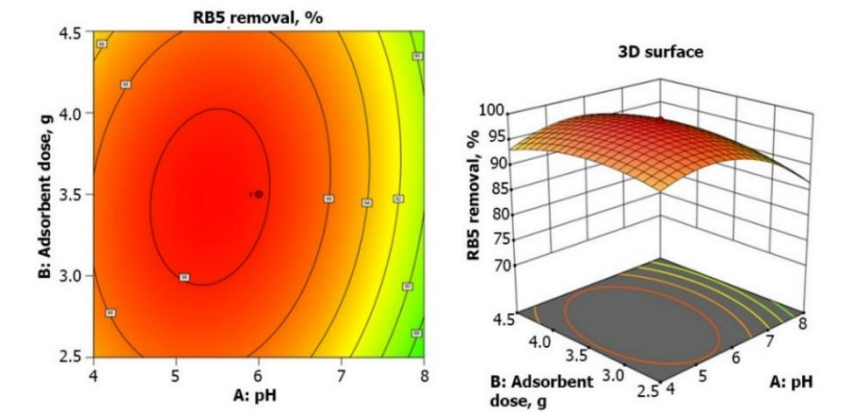


Figure 8. Interaction effect of pH and adsorbent dose

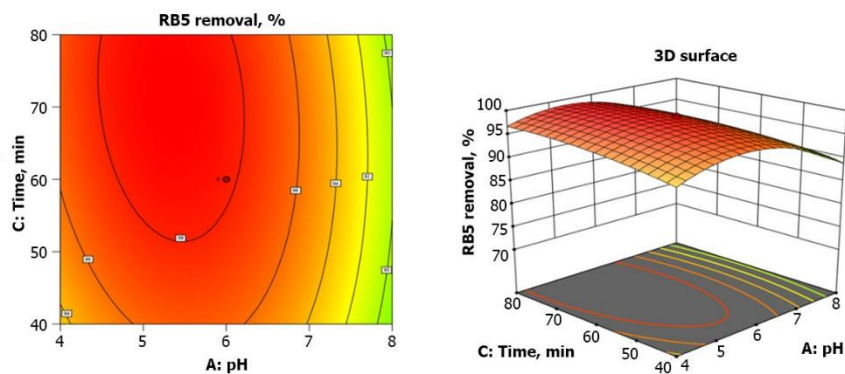


Figure 9. Interaction effect of pH and contact time

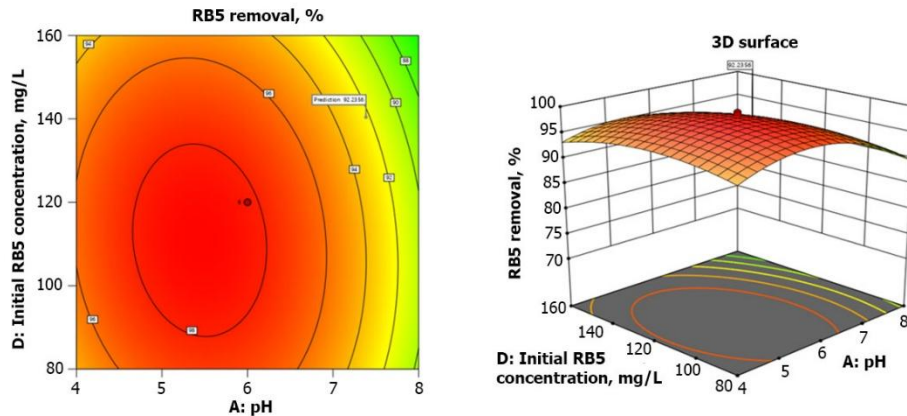


Figure 10. Interaction effect of pH and initial RB5 concentration

### Contact time and Initial RB5 concentration

Figure 11 illustrates how the removal percentage of the CKFC adsorbent changes with varying contact time and RB5 concentration at pH 6, using an adsorbent dose of 3.5 g. The removal percentage increases as the adsorption time extends from 40 to 80 min and as the dye concentration decreases from 160 to 80 mg/L. According to the model's predictions, the removal efficiency gradually rises to 92.8% as the adsorption time reaches 80 min and the RB5 concentration drops to 80 mg/L. This indicates that the initial dye concentration significantly influences the percentage of removal. This higher value of the percentage of removal at lower concentrations suggests that the activated adsorbent has more sorption capacity for RB5.

### Adsorption Phenomenon Study

#### Adsorption kinetics

The adsorption kinetics of the RB5 onto CKFC are illustrated in Figure 12. In the first 5 min, there was a rapid increase in RB5 adsorption, reaching its maximum. After this initial phase, equilibrium was reached within 30 min. This quick kinetic phenomenon suggests that the adsorption process was influenced by the number of available binding sites on CKFC for the adsorption of the RB5 (Harfaoui et al., 2022). After 30 min, the sorbent surface became saturated with the dye, eventually reaching a state of dynamic equilibrium. In this study, the pseudo-first and pseudo-second order rate equations (Equations 6 and 7, respectively) were employed to conduct a comprehensive analysis of the kinetic parameters associated with the adsorption of RB5 onto KFC. The application of two kinetic models to the equilibrium data concerning the RB5 is depicted in Figures 12a and 12b. The pseudo-second-order

kinetics model was determined to be the most suitable for describing the adsorption kinetics of RB5 on CKFC, as it demonstrated a superior linear regression coefficient ( $R^2 > 0.999$ ) in comparison to the pseudo-first-order model ( $R^2 < 0.6029$ ). There is a significant correlation between the experimental and calculated values of adsorption capacity ( $q_e$ ), reinforcing the credibility of the pseudo-second-order kinetic model. These findings suggest that the concentrations of both the adsorbent and the RB5 play crucial roles in the rate-limiting step of the dye attachment process on CKFC. This observation also implies that dye uptake onto activated carbon occurs via a chemisorption mechanism (Mustapha et al., 2020; Sarma et al., 2019). The results of our study are in line with those previously reported as (Khunjan & Kasikamphaiboon, 2021) used a pseudo-second-order model for the treatment of reactive azo dye wastewater using activated kaolin clay.

#### Adsorption isotherms

An adsorption isotherm provides valuable insights into loading capacity, binding affinity, and the surface properties of the adsorbent, which help in understanding the binding mechanism between the adsorbate and the adsorbent. The two popular mathematical models, Langmuir and Freundlich isotherms, were used to analyse the adsorption behaviour of CKFC for the uptake of RB5, as illustrated in Figures 13a and 13b. The Langmuir isotherm assumes that dye wastewater adsorbs onto the KFC surface in a monolayer, suggesting there is a limited number of adsorption sites available. In contrast, The Freundlich equation is an empirical model that considers the adsorption surface of the adsorbent material to be heterogeneous, indicating that there are multiple distinct adsorption sites with varying sorption energy (Çelebi, 2019; Seleman et al., 2023).

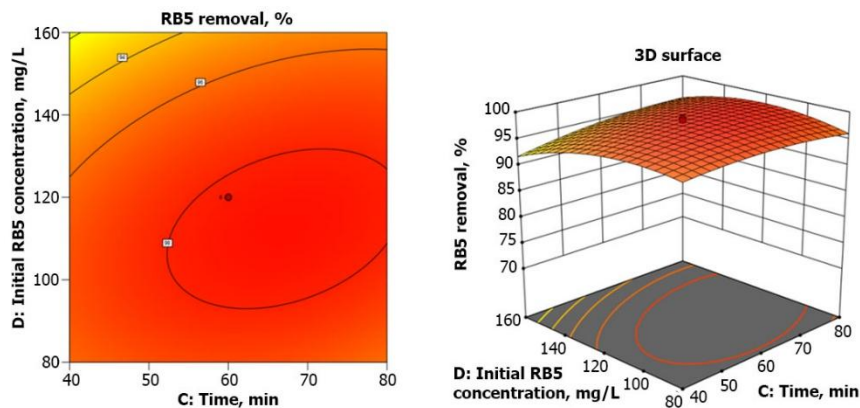


Figure 11. Interaction effect of contact time and initial RB5 concentration

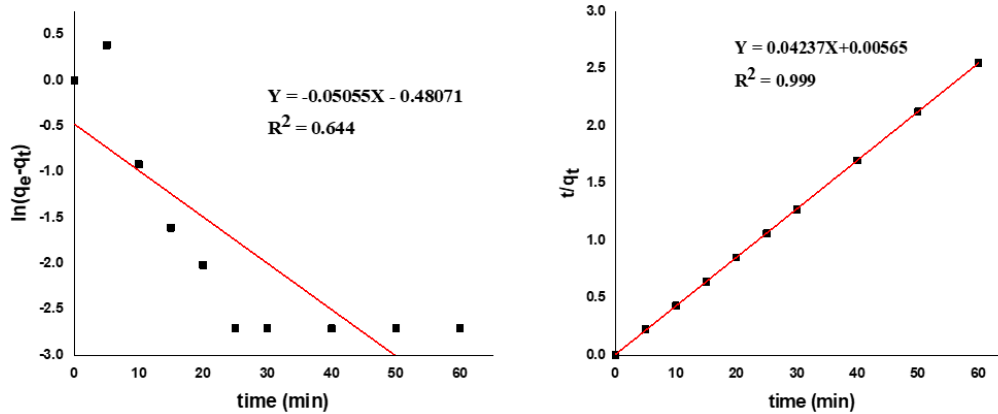


Figure 12. The adsorption kinetics of the RB5 onto CKFC: a – the fitting of PFO kinetic model; b – the fitting of PSO kinetic model

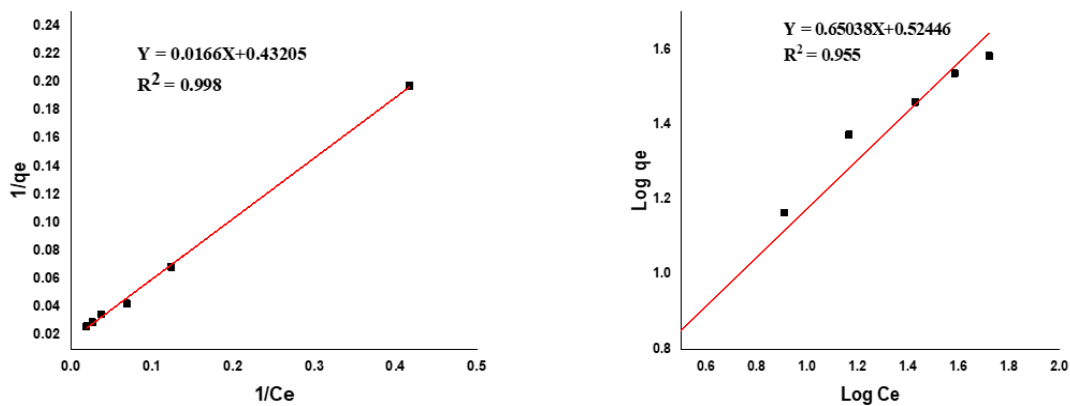


Figure 13. Adsorption isotherms: a – Langmuir isotherm; b – Freundlich's isotherm

The results presented in Figure 13a show that the Langmuir model is the best fit for the data, as indicated by a linear regression coefficient ( $R^2$ ) greater than 0.998. This value greatly exceeds that of the Freundlich isotherm, which has an  $R^2$  value of over 0.955. This finding confirms the monolayer adsorption of RB5 on CKFC. The maximum

sorption capacity of CKFC for RB5 is 60.24 mg/g. Additionally, the separation factor ( $RL$ ) values for CKFC  $< 1$ , which indicates that the adsorption process is favoured. A comparison of the RB5 adsorption capacity of RB5 with CKFC and other bio-sorbents documented in the literature is shown in Table 6.

Table 6. Comparison of the adsorption capacity of CKFC towards RB5s with different ACs

Adsorbents	Dye	$q_{max}$ , mg/g	References
Residue from the aluminium industry	RB5	0.98	Jalali Sarvestani & Doroudi, 2020
NaOH-treated activated sludge	RB5	118.2	Vojnović et al., 2022
Beneficiated Kaolin	BY 28	1.896	Aragaw & Angerasa, 2020
Natural untreated clay	BY 28	76.92	Azha et al., 2021
Calcinated kaolin filter cake	RB5	60.24	This Study

### Regeneration of adsorbent

In this investigation, KFC was regenerated five times using a 0.1 M HCl solution. Figure 14 illustrates the results of washing the RB5-loaded adsorbent with 0.1 M HCl in each cycle. The adsorption efficiency of activated carbon (AC) remained largely unchanged during the first and second recycling processes. However, after the third regeneration phase, the adsorption efficiency of AC significantly decreased for RKFC and showed a moderate decrease for CKFC. Unfortunately, the removal efficiency of KFC dropped from 98.24% to 60.52% for CKFC and from 92.53% to 46.25% for RKFC after five cycles. Compared to RKFC, the CKFC adsorbents demonstrated better adsorption and regeneration efficiency. Considering the availability of raw materials and ease of use, KFC can be regarded as a potential alternative adsorbent for practical applications (Mustapha et al., 2020).

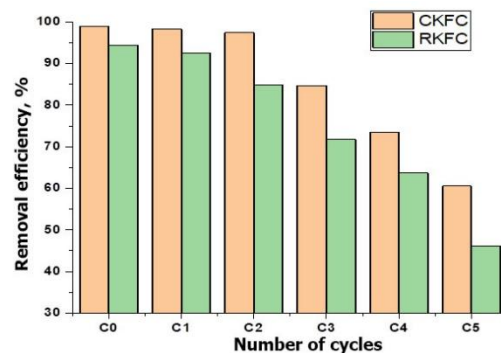


Figure 14. RB5 removal (%) with RKFC and CKFC adsorbent as a function of regeneration cycles

## CONCLUSION

Our environment is significantly impacted by contaminated wastewater from textile industries. Utilizing natural resources, specifically clay-based adsorbents for dye removal, presents a cost-effective alternative. Kaolin filter cake (KFC), an abundant industrial by-product, has shown improved adsorption results after modification. Removal studies have demonstrated KFC's excellent performance in eliminating reactive blue 5 dye. The dye removal process is notably affected by factors such as contact time, pH, initial dye concentration, and the dosage of adsorbent. The optimal pH for KFC in removing RB5 from dye wastewater was found to be 6, with equilibrium achieved after 60 min of contact time. The Langmuir isotherm model indicated substantial sorption capacity, with a maximum of 60.24 mg/g. The experimental data showed the best alignment with the pseudo-second-order kinetic model. Isotherm analysis confirmed a monolayer adsorption mechanism, indicating that the Langmuir model accurately describes the adsorption of RB5 onto KFC. With a high  $R^2$  correlation coefficient of 0.99, the ANOVA response highlights the reliability of the data. Additionally, KFC demonstrated excellent removal performance and can be reused for five cycles. Consequently, kaolin filter cake from industrial solid waste represents a practical, affordable, and locally accessible method for treating coloured industrial wastewater. It is also suitable for expanding to an industrial scale and is an eco-friendly material for environmental restoration.

## Author's statements

### Contributions

Conceptualization: E.A.; Data curation: A.B.; Formal Analysis: A.B.; Investigation: A.B.; Methodology: A.B.; Project administration: E.A.; Resources: A.B.; Software: A.B.;

Supervision: Z.W.N., E.A.; Validation: E.A.; Visualization: A.B., E.A.; Writing – original draft: A.B.; Writing – review & editing: A.B., Z.W.N., E.A.

### Declaration of conflicting interest

The authors declare no competing interests.

### Financial interests

The authors declare they have no financial interests.

### Funding

Not applicable.

### Data availability statement

All relevant data are available within the article and its supporting information file. Additional data related to this article may be requested from the authors.

### AI Disclosure

The authors declare that generative AI was not used to assist in writing this manuscript.

### Ethical approval declarations

Not applicable.

### Additional information

#### Publisher's note

Publisher remains neutral with regard to jurisdictional claims in published maps and institutional affiliations.

The initial version of the research manuscript was published as a preprint:

<https://www.researchsquare.com/article/rs-5651884/v1>.

## REFERENCES

- Abdu, M., Babae, S., Worku, A., Msagati, T. A., & Nure, J. F. (2024). The development of Giant reed biochar for adsorption of Basic Blue 41 and Eriochrome Black T. azo dyes from wastewater. *Scientific Reports*, 14(1), 18320. <https://doi.org/10.1038/s41598-024-67997-5>.
- Abewaa, M., Mengistu, A., Takele, T., Fito, J., & Nkambule, T. (2023). Adsorptive removal of malachite green dye from aqueous solution using Rumex abyssinicus derived activated carbon. *Scientific Reports*, 13(1), 14701. <https://doi.org/10.1038/s41598-023-41957-x>.
- Adamu, A. (2008). Adsorptive removal of reactive azo dyes using industrial residue. *Addis Ababa University*. Available: <http://thesisbank.jhia.ac.ke/4509/>.
- Alemayehu, E., Melak, F., Sharma, S. K., Van der Bruggen, B., & Lennartz, B. (2017). Use of porous volcanic rocks for the adsorptive removal of copper. *Water and Environment Journal*, 31(2), 194–201. <https://doi.org/10.1111/wej.12234>.
- Alnasrawy, S. T. (2023). Adsorption Efficiency, Isotherms, and kinetics for cationic dye removal using Biowaste Adsorbent. *Journal of Hazardous, Toxic, and Radioactive Waste*, 27(1), 04022040. [https://doi.org/10.1061/\(ASCE\)HZ.2153-5515.0000735](https://doi.org/10.1061/(ASCE)HZ.2153-5515.0000735).
- Amin, M. T., Alazba, A. A., & Shafiq, M. (2015). Adsorptive removal of reactive black 5 from wastewater using bentonite clay: isotherms, kinetics and thermodynamics. *Sustainability*, 7(11), 15302–15318. <https://doi.org/10.3390/su71115302>.
- Angerasa, F. T., Kalifa, M. A., Jembere, A. L., & Genet, M. B. (2021). Spent kaolin filter cake as an effective adsorbent for the removal of Hexavalent Chromium [Cr (VI)] from aqueous solution: Comparative study of wastewater treatment methods. *South African Journal of Chemical Engineering*, 38(1), 90–103. <https://hdl.handle.net/10520/ejc-chemeng-v38-n1-a10>.
- Aragaw, T. A. (2020). The effect of mechanical treatment and calcination temperature of Ethiopian kaolin on amorphous metakaolin product. In *Advances of Science and Technology: 7th EAI International Conference, ICAST 2019, Bahir Dar, Ethiopia, August 2–4, 2019, Proceedings 7* (pp. 662–671). Springer International Publishing. [https://doi.org/10.1007/978-3-030-43690-2\\_50](https://doi.org/10.1007/978-3-030-43690-2_50).
- Aragaw, T. A., & Alene, A. N. (2022). A comparative study of acidic, basic, and reactive dyes adsorption from aqueous solution onto kaolin adsorbent: Effect of operating parameters, isotherms, kinetics, and thermodynamics. *Emerging Contaminants*, 8, 59–74. <https://doi.org/10.1016/j.emcon.2022.01.002>.
- Aragaw, T. A., & Angerasa, F. T. (2020). Synthesis and characterization of Ethiopian kaolin for the removal of basic yellow (BY 28) dye from aqueous solution as a potential adsorbent. *Heliyon*, 6(9). <https://doi.org/10.1016/j.heliyon.2020.e04975>.
- Aragaw, T. A., & Kuraz, F. (2018, October). Physico-chemical characterizations of Ethiopian kaolin for industrial applications: case study WDP propoxur formulations. In *International Conference on Advances of Science and Technology* (pp. 122–134). Cham: Springer International Publishing. [https://doi.org/10.1007/978-3-030-15357-1\\_10](https://doi.org/10.1007/978-3-030-15357-1_10).
- Azha, S. F., Shahadat, M., Ismail, S., Ali, S. W., & Ahammad, S. Z. (2021). Prospect of clay-based flexible adsorbent coatings as cleaner production technique in wastewater treatment, challenges, and issues: A review. *Journal of the Taiwan Institute of Chemical Engineers*, 120, 178–206. <https://doi.org/10.1016/j.jtice.2021.03.018>.
- Bello, A. M., Muhammad, N. A., & Hamisu, A. (2023). RSM Optimized Adsorption of Eriochrome Black T Dye onto Alumina Nanoparticles: Isotherm and Kinetics Studies. *Physical Chemistry Research*, 11(2), 315–326. <https://doi.org/10.22036/pcr.2022.335182.2065>.
- Caponi, N., Collazzo, G. C., Jahn, S. L., Dotto, G. L., Mazutti, M. A., & Foletto, E. L. (2017). Use of Brazilian kaolin as a potential low-cost

- adsorbent for the removal of malachite green from colored effluents. *Materials Research*, 20(Suppl 2), 14–22. <https://doi.org/10.1590/1980-5373-MR-2016-0673>.
- Carmen, Z., & Daniela, S. (2012). Textile organic dyes-characteristics, polluting effects and separation/elimination procedures from industrial effluents-a critical overview (Vol. 3, pp. 55–86). *Rijeka: IntechOpen*. Available: <https://www.flagshipdhaka.com/water-waste-water/ecr/pdf/22.pdf>.
- Çelebi, H. (2019). The applicability of evaluable wastes for the adsorption of Reactive Black 5. *International Journal of Environmental Science and Technology*, 16(1), 135–146. <https://doi.org/10.1007/s13762-018-1969-3>.
- Das, A., & Mishra, S. (2017). Removal of textile dye reactive green-19 using bacterial consortium: process optimization using response surface methodology and kinetics study. *Journal of Environmental Chemical Engineering*, 5(1), 612–627. <https://doi.org/10.1016/j.jece.2016.10.005>.
- Dutta, S. (2013). Optimization of Reactive Black 5 removal by adsorption process using Box–Behnken design. *Desalination and Water Treatment*, 51(40–42), 7631–7638. <https://doi.org/10.1080/19443994.2013.779597>.
- Erasto, L., Hellar-Kihampa, H., Mgani, Q. A., & Lugwisha, E. H. J. (2023). Absorbance enhancement of a treated Tanzanian kaolin for removal of synthetic dyes from contaminated water. *International Journal of Biological and Chemical Sciences*, 17(6), 2575–2594. <https://doi.org/10.4314/ijbcs.v17i6.34>.
- Eren, Z., & Acar, F. N. (2006). Adsorption of Reactive Black 5 from an aqueous solution: equilibrium and kinetic studies. *Desalination*, 194(1–3), 1–10. <https://doi.org/10.1016/j.desal.2005.10.022>.
- Farrokhzadeh, S., Razmi, H., & Jannat, B. (2020). Study of Reactive Red 195 anionic dye adsorption on calcined marble powder as potential eco-friendly adsorbent. *Human, Health and Halal Metrics*, 1(1), 42–56. <https://doi.org/10.30502/jhhhm.2020.107920>.
- Fito, J., Ebrahim, O., & Nkambule, T. T. (2023). The application Mn-Ni ferrite nanocomposite for adsorption of chromium from textile industrial wastewater. *Water, Air, & Soil Pollution*, 234(1), 37. <https://doi.org/10.1007/s11270-022-06058-x>.
- Gonen, F., & Biçer, G. (2022). Fractal adsorption characteristics and statistical analysis approach of complex dye molecule on metal oxide particles—A case study of Reactive Black 5 (RB 5) adsorption onto NiO nanoparticles. *Open Journal of Nano*, 7(2), 81–93. <https://doi.org/10.56171/ojn.1065924>.
- Hamad, H. N., & Idrus, S. (2022). Recent developments in the application of bio-waste-derived adsorbents for the removal of methylene blue from wastewater: a review. *Polymers*, 14(4), 783. <https://doi.org/10.3390/polym14040783>.
- Hamri, N., Imessaoudene, A., Hadadi, A., Cheikh, S., Boukerroui, A., Bollinger, J. C., ... & Mouni, L. (2024). Enhanced adsorption capacity of methylene blue dye onto kaolin through acid treatment: batch adsorption and machine learning studies. *Water*, 16(2), 243. <https://doi.org/10.3390/w16020243>.
- Harfaoui, S. E., Driouich, A., Mohssine, A., Belouafa, S., Zmirli, Z., Mountacer, H., ... & Chaair, H. (2022). Modelization and optimization of the treatment of the reactive black-5 dye from industry effluents using experimental design methodology. *Scientific African*, 16, e01229. <https://doi.org/10.1016/j.sciaf.2022.e01229>.
- Hasan, M., Al Biruni, M. T., Azad, S., & Ahmed, T. (2024). Adsorptive removal of dye from textile wastewater employing Moringa oleifera leaves biochar as a natural biosorbent. *Biomass Conversion and Biorefinery*, 14(10), 11075–11091. <https://doi.org/10.1007/s13399-022-03196-4>.
- Hassan, A. K., Atiya, M. A., & Mahmoud, Z. A. (2022). Photo-Fenton-like degradation of direct blue 15 using fixed bed reactor containing bimetallic nanoparticles: Effects and Box–Behnken optimization. *Environmental Technology & Innovation*, 28, 102907. <https://doi.org/10.1016/j.eti.2022.102907>.
- Ike, J. I., Babayemi, A. K., Egbosiuba, T. C., Jin, C. G., Mustapha, S., Yusuff, A. S., ... & Igwegbe, C. A. (2024). Treated kaolin clay incorporated with nickel nanoparticles for enhanced removal of crystal violet and methyl orange from textile wastewater. *ACS Applied Engineering Materials*, 2(4), 1031–1046. <https://doi.org/10.1021/acsaenm.4c00065>.
- Ishak, Z., Salim, S. D., & Kumar, D. (2022). Adsorption of methylene blue and reactive black 5 by activated carbon derived from tamarind seeds. *Tropical Aquatic and Soil Pollution*, 2(1), 1–12. <https://doi.org/10.53623/tasp.v2i1.26>.
- Jalali Sarvestani, M. R., & Doroudi, Z. (2020). Removal of reactive black 5 from waste waters by adsorption: a comprehensive review. *Journal of Water and Environmental Nanotechnology*, 5(2), 180–190. <https://doi.org/10.22090/jwent.2020.02.008>.
- Johin, J., Nidheesh, P. V., & Sivasankar, T. (2019). Sono-electro-chemical treatment of reactive black 5 dye and real textile effluent using MnSO<sub>4</sub>/Na<sub>2</sub>S<sub>2</sub>O<sub>8</sub> electrolytes. *Arabian Journal for Science and Engineering*, 44(12), 9987–9996. <https://doi.org/10.1007/s13369-019-04159-0>.
- Kalkan, E., Nadaroğlu, H., Celebi, N., & Tozsın, G. (2014). Removal of textile dye Reactive Black 5 from aqueous solution by adsorption on laccase-modified silica fume. *Desalination and Water Treatment*, 52(31–33), 6122–6134. <https://doi.org/10.1080/19443994.2013.811114>.
- Kassa, A. E., Shibeshi, N. T., Tizazu, B. Z., & Prabhu, S. V. (2022). Characteristic investigations on Ethiopian kaolinite: effect of calcination temperature on pozzolanic activity and specific surface area. *Advances in Materials Science and Engineering*, 2022(1), 2481066. <https://doi.org/10.1155/2022/2481066>.
- Khan, T. A., & Khan, E. A. (2016). Adsorptive uptake of basic dyes from aqueous solution by novel brown linseed deoiled cake activated carbon: equilibrium isotherms and dynamics. *Journal of Environmental Chemical Engineering*, 4(3), 3084–3095. <https://doi.org/10.1016/j.jece.2016.06.009>.
- Khunjan, U., & Kasikamphaiboon, P. (2021). Green synthesis of kaolin-supported nanoscale zero-valent iron using ruellia tuberosa leaf extract for effective decolorization of azo dye reactive black 5. *Arabian Journal for Science and Engineering*, 46, 383–394. <https://doi.org/10.1007/s13369-020-04831-w>.
- Kosmulski, M. (2021). The pH dependent surface charging and points of zero charge. IX. Update. *Advances in Colloid and Interface Science*, 296, 102519. <https://doi.org/10.1016/j.cis.2021.102519>.
- Li, J., Cai, J., Zhong, L., Wang, H., Cheng, H., & Ma, Q. (2018). Adsorption of reactive dyes onto chitosan/montmorillonite intercalated composite: multi-response optimization, kinetic, isotherm and thermodynamic study. *Water Science and Technology*, 77(11), 2598–2612. <https://doi.org/10.2166/wst.2018.221>.
- Li, Y., Chen, Y., Xia, W., & Xie, G. (2021). Filtration of kaolinite and coal mixture suspension: Settling behavior and filter cake structure analysis. *Powder Technology*, 381, 122–128. <https://doi.org/10.1016/j.powtec.2020.12.050>.
- Magdy, A., Fouad, Y. O., Abdel-Aziz, M. H., & Konsowa, A. H. (2017). Synthesis and characterization of Fe<sub>3</sub>O<sub>4</sub>/kaolin magnetic nanocomposite and its application in wastewater treatment. *Journal of Industrial and Engineering Chemistry*, 56, 299–311. <https://doi.org/10.1016/j.jiec.2017.07.023>.
- Mulushewa, Z., Dinbore, W. T., & Ayele, Y. (2021). Removal of methylene blue from textile waste water using kaolin and zeolite-x synthesized from Ethiopian kaolin. *Environmental Analysis, Health and Toxicology*, 36(1), e2021007. <https://doi.org/10.5620/eaht.2021007>.
- Munagapati, V. S., Wen, J. C., Pan, C. L., Gutha, Y., Wen, J. H., & Reddy, G. M. (2020). Adsorptive removal of anionic dye (Reactive Black 5) from aqueous solution using chemically modified banana peel powder: kinetic, isotherm, thermodynamic, and reusability studies. *International Journal of Phytoremediation*, 22(3), 267–278. <https://doi.org/10.1080/15226514.2019.1658709>.

- Mustapha, S., Tijani, J. O., Ndamitso, M. M., Abdulkareem, A. S., Shuaib, D. T., & Mohammed, A. K. (2021). Adsorptive removal of pollutants from industrial wastewater using mesoporous kaolin and kaolin/TiO<sub>2</sub> nanoadsorbents. *Environmental Nanotechnology, Monitoring & Management*, 15, 100414. <https://doi.org/10.1016/j.enmm.2020.100414>.
- Mustapha, S., Tijani, J. O., Ndamitso, M. M., Abdulkareem, S. A., Shuaib, D. T., Mohammed, A. K., & Sumaila, A. J. S. R. (2020). The role of kaolin and kaolin/ZnO nanoadsorbents in adsorption studies for tannery wastewater treatment. *Scientific Reports*, 10(1), 13068. <https://doi.org/10.1038/s41598-020-69808-z>.
- Mutambyi, V., Jean Nepo, H., Rugabirwa, B., Kwisanga, C., Beakou, B. H., Munyegaju, J., ... & Mushirabwoba, B. (2023). Removal of Reactive Black 5 from simulated textile effluents by an electrocoagulation process: optimization by response surface methodology. *Water Practice & Technology*, 18(12), 3048–3064. <https://doi.org/10.2166/wpt.2023.210>.
- Njuhous, S., Mouafon, M., Pountouenchi, A., Njindam, O. R., Lecomte-Nana, G. L., & Njoya, D. (2023). Rice husks and kaolin based ceramic membrane for filtration of slaughterhouse wastewater: optimization study using response surface methodology (RSM) and responses interdependence analysis. *Transactions of the Indian Ceramic Society*, 82(2), 143–155. <https://doi.org/10.1080/0371750X.2023.2205601>.
- Nure, J. F., Mengistu, A., Abewaa, M., Angassa, K., Moyo, W., Phiri, Z., ... & Nkambule, T. T. (2023). Adsorption of Black MNN reactive dye from tannery wastewater using activated carbon of Rumex Abyssinicus. *Journal of the Taiwan Institute of Chemical Engineers*, 151, 105138. <https://doi.org/10.1016/j.jtice.2023.105138>.
- Obaid, F. H., & Ali, L. A. M. (2023, February). Adsorption of the textile dye (reactive black 5) using orange peels as an adsorbent low-cost. In *AIP Conference Proceedings* (Vol. 2414, No. 1). AIP Publishing. <https://doi.org/10.1063/5.0115736>.
- Ribeiro, A. C., Barbosa de Andrade, M., Quesada, H. B., Bergamasco Beltran, L., Bergamasco, R., Calado Santos Sobral da Fonseca, M. M., & da Costa Neves Fernandes de Almeida Duarte, E. (2022). Physico-chemical and electrostatic surface characterisation of mica mineral and its applicability on the adsorption of Safranin Orange and Reactive Black 5 dyes. *Environmental Technology*, 43(24), 3765–3778. <https://doi.org/10.1080/09593330.2021.1934562>.
- Sarma, G. K., Sen Gupta, S., & Bhattacharyya, K. G. (2019). Removal of hazardous basic dyes from aqueous solution by adsorption onto kaolinite and acid-treated kaolinite: kinetics, isotherm and mechanistic study. *SN Applied Sciences*, 1, 1–15. <https://doi.org/10.1007/s42452-019-0216-y>.
- Seleman, M., Sime, T., Ayele, A., Sergawie, A., Nkambule, T., & Fito, J. (2023). Isotherms and kinetic studies of copper removal from textile wastewater and aqueous solution using powdered banana peel waste as an adsorbent in batch adsorption systems. *International Journal of Biomaterials*, 2023(1), 2012069. <https://doi.org/10.1155/2023/2012069>.
- Slatni, I., Elberichi, F. Z., Duplay, J., Fardjaoui, N. E. H., Guendouzi, A., Guendouzi, O., ... & Rekkab, I. (2020). Mesoporous silica synthesized from natural local kaolin as an effective adsorbent for removing of Acid Red 337 and its application in the treatment of real industrial textile effluent. *Environmental Science and Pollution Research*, 27, 38422–38433. <https://doi.org/10.1007/s11356-020-08615-5>.
- Souhassou, H., Fahoul, Y., El Mrabet, I., Iboustaten, E., Assila, O., Nahali, L., ... & Kherbeche, A. (2024). Optimization of basic red 29 dye removal onto a natural red clay using response surface methodology. *Journal of the Iranian Chemical Society*, 21(1), 275–291. <https://doi.org/10.1007/s13738-023-02924-5>.
- Srivastava, A., Rani, R., & Kumar, S. (2022). Optimization, kinetics, and thermodynamics aspects in the biodegradation of reactive black 5 (RB5) dye from textile wastewater using isolated bacterial strain, Bacillus albus DD1. *Water Science and Technology*, 86(3), 610–624. <https://doi.org/10.2166/wst.2022.212>.
- Vojnović, B., Cetina, M., Franjković, P., & Sutlović, A. (2022). Influence of initial pH value on the adsorption of reactive black 5 dye on powdered activated carbon: kinetics, mechanisms, and thermodynamics. *Molecules*, 27(4), 1349. <https://doi.org/10.3390/molecules27041349>.
- Worku, Z., Tibebe, S., Nure, J. F., Tibebe, S., Moyo, W., Ambaye, A. D., & Nkambule, T. T. (2023). Adsorption of chromium from electroplating wastewater using activated carbon developed from water hyacinth. *BMC Chemistry*, 17(1), 85. <https://doi.org/10.1186/s13065-023-00993-4>.